Epitope Mapping of the Transforming Growth Factor-β Superfamily Protein, Macrophage Inhibitory Cytokine-1 (MIC-1): Identification of at Least Five Distinct Epitope Specificities[†]

W. Douglas Fairlie, Patricia K. Russell, Wan M. Wu, Anthony G. Moore, Hong-Ping Zhang, Peter K. Brown, Asne R. Bauskin, and Samuel N. Breit*

Centre for Immunology, St. Vincent's Hospital and University of New South Wales, Victoria St, Sydney, New South Wales, Australia, 2010

Received May 10, 2000; Revised Manuscript Received August 14, 2000

ABSTRACT: Macrophage inhibitory cytokine-1 (MIC-1) is a divergent member of the transforming growth factor-β (TGF-β) superfamily whose increased expression is associated with macrophage activation and which is expressed highly in placenta as compared to other tissues. There are two known allelic forms of human MIC-1 due an amino acid substitution at position 6 of the mature protein. We have raised four monoclonal antibodies (MAbs) and one polyclonal antiserum to the mature protein region of human MIC-1 and have used an extensive panel of MIC-1 relatives, mutants, and chimeras to map their epitopes. None of the MAbs were able to cross-react with either the murine homologue of MIC-1 or with hTGF-β1, and all of the MAb epitopes were conformation-dependent. A distinct cross-reactivity pattern with the various antigens was observed for each of the monoclonal and polyclonal antibodies suggesting the presence of at least five immunogenic regions on the MIC-1 surface. One of the MAbs is directed against the amino terminus of the protein and can distinguish between the two allelic forms of MIC-1. The epitopes for the other three MAbs were located near the tips of the so-called "fingers" of the protein and appeared to be partially overlapping as each involved amino acids in the region 24−37. In one case, it was possible to mutate murine MIC-1 so that it could be recognized by one of the MAbs. Finally, the use of another mutant in which Cys 77 was replaced by serine enabled confirmation of the location of the MIC-1 interchain disulfide bond.

Macrophage inhibitory cytokine-1 (MIC-1)[1] is a divergent member of the transforming growth factor-β (TGF-β) superfamily first cloned in this laboratory (*1*, *2*). It has been variously reported to inhibit TNF-alpha production from lipopolysaccharide stimulated macrophages (*1*), induce cartilage formation and the early stages of endochonadal bone formation, (*3*) and inhibit proliferation of primitive haemopoietic progenitors (*4*). A recent report suggested that MIC-1 can also suppress tumor cell growth in vitro (*5*). However, very high concentrations of the protein were required to elicit this latter effect, suggesting that this is not the primary role of MIC-1 in vivo. Finally, the very high expression of the protein in the placenta suggests that MIC-1 may be important for placental function and/or fetal development.

As with all TGF-β superfamily members, MIC-1 is synthesized with a long propeptide region (*1*). Following processing of the protein at a furin-like cleavage site, the mature protein is secreted as a disulfide-linked homodimer. The mature protein subunits contain the conserved pattern of seven cysteine residues which is a hallmark of TGF-β superfamily proteins. In the members of this superfamily for which a three-dimensional structure has been solved, six of these cysteines form three intrachain disulfide bridges that are arranged into a cystine-knot motif (*6*−*11*). An additional pair of cysteine residues is found close to the amino-terminus of the mature MIC-1 protein. In TGF-β1,2 and 3, the corresponding residues form a fourth intrachain disulfide bond that links the amino terminus to the core of the protein.

The three-dimensional structures have been determined for the three mammalian isoforms of TGF-β (TGF-β1,2 and 3) (*6*, *8*, *9*), two members of the bone morphogenetic subfamily (BMP-2 and BMP-7) (*7*, *11*) as well as for the more divergent glial-derived neutrotropic factor (GDNF) (*10*). All have a highly conserved subunit structure that has been described as an outstretched hand with two slightly curled antiparallel beta sheet "fingers" extending from an alpha helical "heel" region (*6*). The strong conservation of the subunit structure between family members, despite low sequence homology, is illustrated in Figure 1.

A number of recent reports have made significant contributions to the understanding of some of the structure−function relationships for specific superfamily members. In

[†] This work has been funded in part by grants from St. Vincent's Hospital and by Meriton Apartments Pty Ltd through an R&D syndicate arranged by Macquarie Bank Limited. In addition, this project was partially funded by a New South Wales Health Research and Development infrastructure grant.

* To whom correspondence should be addressed.

[1] Abbreviations: BMP: bone morphogenetic protein; CHO: Chinese hamster ovary cells; FBS: fetal bovine serum; GDNF: Glial-derived neurotropic factor; hCG: human chorionic gonadotrophin; MAb: monoclonal antibody; MIC-1: macrophage inhibitory cytokine-1; PAb: polyclonal antibody; RIA: radioimmunoassay; TGF-β: transforming growth factor-β.

10.1021/bi001064p CCC: $20.00
Published on Web 12/07/2000

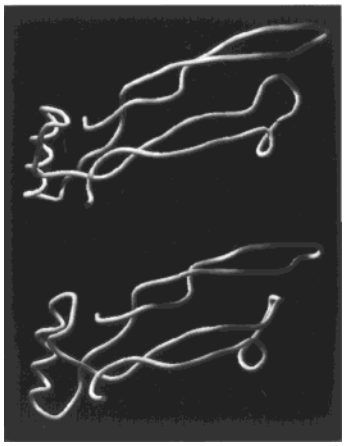

FIGURE 1: Conservation of TGF-β superfamily subunit structure. The three-dimensional carbon backbone structures for (top) BMP-7 (derived from PDB file 1 BMP) and (bottom) hTGF-β1 (PDB file 1KLA) show strong conservation of overall structure despite low sequence identity (26%). Figure was created using the Swiss PDB viewer program.

particular, key receptor binding residues or regions have been identified for TGF-β1 and TGF-β2 (*12*, *13*), activin A (*14*), and GDNF (*15*, *16*). However, no systematic study mapping the antigenic determinants on any superfamily member has yet to appear. This is in part due to difficulties in raising antibodies to superfamily members such as TGF-β which have highly conserved protein sequences between species and which also have immunosuppressive activity (*17*).

Most studies in which antibodies against TGF-β superfamily cytokines have been characterized have utilized anti-peptide antibodies (*5*, *13*, *18*−*24*), although some anti-protein monoclonal antibodies (MAbs) have also been described (*25*−*27*). The majority of the above reports have concentrated on determining the ability of the antiserum to neutralize biological activity of a particular cytokine or the suitability of the antiserum for use in cytokine-specific assays. There are very few reports in which epitope specificities for MAbs raised against whole TGF-β-superfamily proteins have been determined (*28*) or attempted to be determined (*25*). In the present paper, we have undertaken a study directed at gaining an insight into the immunogenicity of a TGF-β superfamily protein by mapping the epitopes for four MAbs that we have raised against the human MIC-1 mature protein. This is the first study in which the surface structure of MIC-1 has been systematically examined. The results suggest that major regions of immunogenicity on MIC-1 coincide with known receptor binding sites on other TGF-β superfamily cytokines.

EXPERIMENTAL PROCEDURES

Cell Culture. Chinese hamster ovary cells (CHO-K1) were maintained as recommended by the American Type Culture Collection in DMEM/F12 medium supplemented with 5% (v/v) fetal bovine serum (FBS). For collection of conditioned medium for immunoprecipitation and Western blotting experiments, transfected cells were cultured in the absence of FBS (see below).

Antibodies. Monoclonal antibody secreting hybridomas 13, 26, 10, and 14 were raised by immunization of BALB/c mice with recombinant human MIC-1 that was produced in *Pichia pastoris* as described previously (*29*). Hybridomas were cultured in DMEM (Gibco BRL) medium containing 4.5 g/L D-glucose, 110 mg/L sodium pyruvate, 0.584 g/lL L-glutamine, and 4 mg/L pyridoxine hydrochloride and supplemented with 20% (v/v) FBS (CSL Melbourne). For MAb collection, the hybridomas were transferred into fresh DMEM-hi glucose supplemented with Nutridoma-SR (Boehringer Mannheim) for 7 days. The culture supernatants were centrifuged at 2000 rpm for 10 min to remove cell debris then frozen until used. The polyclonal antiserum 233 was raised in sheep by immunization with the same recombinant protein. The particular antiserum used in this study was obtained following the fourth monthly bleed. Anti-FLAG M2 antibody coupled to agarose used in immunoprecipitations was purchased from Sigma.

Radio-Immuno Assay. The radio-immuno assay (RIA) was performed as described previously (*29*) and involved competition between radio-phosphorylated hMIC-1 and increasing concentrations of unlabeled recombinant hMIC-1 with each antibody. The MAb supernatant dilutions used were MAb 26: 1:800; MAb 13: 1:300; MAb 14: 1:40; MAb 10: 1:30. Polyclonal antibody 233 was used at a 1:200 000 dilution.

Preparation of cDNA Constructs. The method for the preparation of the base FLAG-tagged MIC-1 constructs has been described previously (*1*). A FLAG-tagged TGF-β1 construct was also made using a similar method. In each case, the FLAG epitope was engineered onto the amino terminus of the mature peptide of all constructs (i.e., inserted immediately after the furin-like cleavage sequence of propeptide region) to facilitate immunoprecipitation of the secreted proteins. A unique *Eco*RI restriction site was also added immediately before the FLAG epitope to enable subcloning between vectors. The relevant constructs were either cloned into the pOCUS-2 vector (Novagen) for the construction of the chimeras or the pIRES2-EGFP vector (Clontech) for transfection into CHO cells.

Most of the chimeric constructs were made using a whole plasmid PCR technique similar to that described by Fisher and Pei (*30*) but without the *Dpn*I digestion step which was found to be unnecessary. Forward and reverse primers were phosphorylated using T4 polynucleotide kinase (Boehringer Mannheim) before use in PCR. In the case of the human MIC-1/human TGF-β1 (hMIC-1 mature peptide with introduced hTGF-β1 sequences), human MIC-1/murine MIC-1 (hMIC-1 mature peptide with introduced mMIC-1 sequences) or murine MIC-1/human MIC-1 (mMIC-1 mature peptide with introduced hMIC-1 sequences) chimeras, the primers were designed with 3′ sequences complementary to h/mMIC-1 sequences with which to anneal to the template followed by additional bases coding for the sequences that were to be introduced into the construct (see Table 1 for all oligonucleotide sequences). Generally, half of each sequence region to be interchanged for the corresponding TGFβ1/mMIC-1/hMIC-1 sequence was encoded on each (i.e., forward and reverse) primer. The primers used were as follows: hMIC-1/hTGF-β1 site 2: primers 4 and 5; site 3: primers 6 and 7; site 4: primers 8 and 9; site 5: primers 10 and 11; hMIC-1/mMIC-1 site 5: primers 12 and 13; mMIC-1/hMIC-1 site 1: primers 14 and 15; site 5: primers 16 and 17. For the hMIC-1/hTGF-β1 site 2, site 3, and site 5 chimeras with the Cys 77 to Ser mutation, primers 20 and 21 were used on the hMIC-1/hTGF-β1 site 2, 3, and 5 chimera templates in the

Table 1: Oligonucleotide Sequences for Primers Used in PCRs for the Creation of the Various Constructs[a]

primer no.	oligonucleotide sequence
1	**GCTTCAGCTCCACGGAGAAGAAC**TGCTGCCGTCTG(F)
2	**GCATATGCGCGCGACACCAACTACTGCTTCAGCTCC**(F)
3	*ACGATAGATC*TCCGCGGTCATATGCAGTGGCAGTC (R)
4	**AAGTGGATCCACGAGCCCAAG**GAGGTGCAAGTGACC (F)
5	**CCAGCCGAGGTCCTTGCGGAA**CGACGCGCGGACCG (R)
6	**TGGCCCTGTACAACCAGCAT**AAGCCCGACACGGTGCC(F)
7	**GGACCTTGCTGTACTGCGT**TGCCGCCCGGAACTGGC(R)
8	**GCGCCTCG**CCAGCGCCCTGCTGCGTG(F)
9	**CCGGGTT**CAGGCGGTGCAGGCTCGTC(R)
10	**CAAGCCCAAG**GTCCAGACCTATG (F)
11	**CGGCCCACGTA**TTGAATGAGCACC (R)
12	GACCGAC**AGT**GGGGTGTCGCTCCAGACC(F)
13	**CTGTG**AATGAGCACCATGGGATTGTAGC(R)
14	*NNNNNN*GCGCGC**AACGGGGACCAC**TGCCCACTGGGTCCGG(F)
15	*CGG*GGATCCGGCGGCCGCTCAAGCGCAGTGGC(R)
16	GACAGAC**ACC**GGTGTGTCACTGCAGACTTATG(F)
17	**TTTTG**AATAAGAACCACCGGGGTGTAGCTGG (R)
18	CCAGCGCCCT**C**CTGCGTGCCC
19	AACGGGGAC**G**ACTGTCCGCTC
20	**C**TGCGTGCCCGCCAGCTACAATCCCA
21	GAGGGCGCTGGCACCGTGTCGGGCTT

[a] The (F) and (R) after each sequence indicates whether the primer used is a forward or reverse primer, respectively. The bold lettering indicates bases substituted in the construction of chimeras or mutants. Underlined bases indicate restriction sites used or added for cloning. Italicized letters represent additional sequences added to the primer to ensure efficient restriction enzyme digestion.

pOCUS-2 vector. Following PCR and agarose gel purification, the linearized plasmids were recircularized using T4 ligase (Boehringer Mannheim) then transformed in *E. coli*. Plasmid DNA derived from individual colonies was bidirectionally sequenced to confirm that the correct insert had been created. The *Eco*RI/*Sac*II fragment from wild-type MIC-1 in the pIRES2-EGFP vector was then replaced with the same fragment from the each of the mutated constructs in the pOCUS-2 vector.

The only chimeric constructs not made using the above technique were the hMIC-1/TGFβ1 site 1 chimera and the mMIC-1/hMIC-1 site 1 chimera. Both of these were made by direct PCR of mature wild-type MIC-1 insert in pIRES-2-EGFP. In the case of the MIC/TGFβ chimera, two successive rounds of PCR were performed with the common reverse primer 2. In the first round of PCR, the forward primer was primer 1. The product of this PCR was then amplified using primer 2 as the forward primer. For the mMIC-1/hMIC-1 site 1 chimera, the forward primer was primer 14, and the reverse primer was primer 15. The *Bss*HII/*Sac*II fragment of the pIRES2-EGFP vector containing wt MIC-1 was then replaced with the above PCR products digested with the same enzymes.

The two constructs with point mutations, hMIC-1(C77S) (hMIC-1 with Cys 77 substituted for Ser) and hMIC-1 (H6D) (human MIC-1 with His 6 substituted for Asp) were both made using the Altered Site II mutagenesis kit (Promega) which was performed essentially as per the manufacturer's instructions using the mutagenenic oligonucleotides 18 and 19, respectively.

Transfections. Transient transfections were performed in CHO-K1 cells grown in 6-well plates to 60−80% confluence using lipofectamine (Gibco BRL) as per the manufacturer's instructions. After overnight incubation at 37 °C, the cells were washed with DMEM/F12 medium containing 5% (v/v) FBS and incubated for 6 h at 37 °C in the same medium. Cells were washed with serum-free medium and then maintained in 1 mL of the same medium for a further 48 h before collection for immunoprecipitation and Western blot analysis. Transfection efficiency was monitored using a fluorescent microscope that could detect the enhanced green fluorescent protein, a product of the pIRES2-EGFP vector, and was routinely in the order of 60−80%. Comparison between supernatants was only made from wells in which the cells were transfected to approximately the same degree.

Immunoprecipitation, SDS−PAGE, and Western Blotting. Immunoprecipitation of the FLAG-tagged proteins in the conditioned medium was performed by addition of 10 μL of agarose beads coated with the anti-FLAG antibody, then overnight incubation at 4 °C. The bound proteins were then washed three times with phosphate-buffered saline and eluted by heating at 95 °C for 5 min in SDS−PAGE sample buffer with (reducing) or without (nonreducing) 2-mercaptoethanol.

Western blot analysis was performed as described previously (*1*). Membranes were probed with either the sheep anti-MIC-1 polyclonal antiserum 233 (diluted 1:7000) or the murine MAb culture supernatants [diluted 1:1 with phosphate-buffed saline containing 2% (w/v) bovine serum albumin and 0.1% (v/v) Tween-20] followed by either biotinylated anti-sheep (1:1000) (Sigma) or anti-mouse antiserum (1:1000) (Amersham), respectively. Blots were then visualized on film after treatment with strepavidin-horseradish peroxidase conjugate (Amersham) and chemiluminescence reagents (NEN).

RESULTS AND DISCUSSION

Construct Design and Analysis Rationale. In this study, we have aimed to map the epitopes for four monoclonal antibodies and one polyclonal antiserum, all of which were raised against recombinant human MIC-1. The specificity of each antibody was determined by Western blot analysis using a panel of antigens including hMIC-1, mMIC-1, hTGF-β1, as well as hMIC-1/hTGF-β1, hMIC-1/mMIC-1, and mMIC-1/hMIC-1 chimeras. The rationale behind the use of chimeras was based upon the very strong conservation of

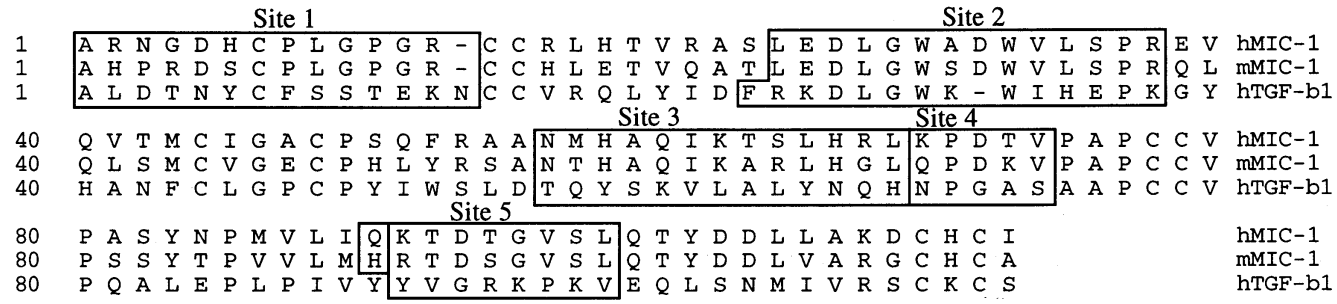

FIGURE 2: Sequence alignment of hMIC-1, mMIC-1, and hTGF-β1 mature peptides. Boxed regions indicate the five sites replaced in hMIC-1 with either hTGF-β1 or mMIC-1 sequences. The extended box at the amino terminal end of site 5 indicates the extra residue replaced in the hMIC-1/mMIC-1 and mMIC-1/hMIC site 5 chimeras.

the three-dimensional structure of TGF-β superfamily proteins despite relatively low sequence homology (*6*−*11*). For example, hTGF-β1 and BMP-7 are only 26% identical, yet they have a remarkably similar three-dimensional structures (Figure 1). Therefore, it was anticipated that primary structural changes could be made that would allow the epitopes to be mapped while also maintaining the conformation of the molecules so that they would fold correctly and be secreted.

In the case of the MIC-1/TGF-β chimeras, five distinct regions of MIC-1 were replaced with the corresponding region of hTGF-β1. Site 2 (residues 24−37) and site 5 (residues 91−98) correspond to surface-exposed loop regions of TGF-β1 and form the tips of the so-called "fingers" (see Figure 2 for sequences of each region and Figure 5, panel a, for relative location of each region on TGF-β). Site 1 (residues 1−13) corresponds to the amino terminus, which in TGF-β1 forms a short, mostly surface-exposed α-helix. Site 3 (residues 56−68) corresponds to the major α-helix in TGF-β, the inner surface of which is buried in the dimer interface while the outer surface is predominantly surface exposed. The site 3 α-helix terminates in a type II β-turn (residues 69−73) which corresponds to site 4. In the mMIC-1/hMIC-1 chimeras, part of site 1 (residues 2−6) and site 5 (plus residue H90) of mMIC-1 were replaced with the corresponding region of hMIC-1 while another construct was made with site 5 (plus residue Q90) of hMIC-1 replaced with the corresponding region of mMIC-1. These murine/human constructs were made to further refine the epitope structures.

To determine whether the epitopes were linear or conformationally dependent, MIC-1 in which the disulfide bonds had been reduced was used. In addition, a construct was made in which the cysteine residue, Cys 77, predicted to form an interchain disulfide bond was mutated to a serine, thereby preventing dimer formation. This made it possible to determine if any epitopes extended across both subunits within the MIC-1 dimer, or whether the conformation of the protein/epitopes changed upon dimerization.

Finally, two alleles for MIC-1 have been reported that are polymorphic at position 6 of the mature peptide region (*4*, *31*). In one case, the amino acid residue at this position is histidine, while in the other allele it is aspartic acid. This substitution occurs within site 1 described above. We initially identified a number of clones in a fetal lung cDNA library with both sequences. Subsequently numerous other cDNA clones with the same variable sequence (and derived from various tissues types) have been deposited in the Expressed

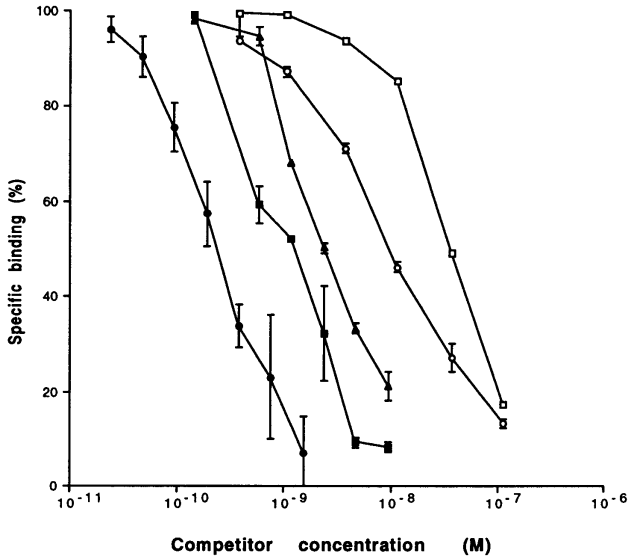

FIGURE 3: MIC-1 radioimmunoassay. ^{32}P-MIC-1 and varying concentrations of unlabeled MIC-1 were incubated with antibodies and immune complexes isolated with Protein G-sepharose. Antibodies used were polyclonal anti-MIC-1 antiserum 233 (●), MAb 26 (■), MAb 13 (▲), MAb 14 (○), MAb10 (□). Points are the mean of duplicate determinations in at least two separate assays.

Sequence Tag database. We therefore wished to determine whether any of the antibodies were allele-specific.

General Characteristics of the Antibodies. Initially, the relative affinity of each antibody for hMIC-1 (which was used as the immunogen) was examined by competitive RIA (Figure 3). It was found that the polyclonal antiserum had the highest affinity for hMIC-1 as judged by its ED50 (2.5×10^{-10} M) while MAbs 26 and 13 had the highest affinities of the monoclonal antibodies with ED50's in the range $1.3-2.5 \times 10^{-9}$ M, respectively. MAbs 10 and 14 bound with about 10-fold less affinity with ED50's in the range $1.0-4.0 \times 10^{-8}$ M.

For every MIC-1-based construct tested in the Western blots, at least one antibody recognized a protein of the correct molecular weight for the FLAG-tagged MIC-1 (monomeric molecular mass approximately 15 kDa or dimeric molecular mass 30 kDa) (Figure 4, rows a−m). This indicates that all of the mutant proteins were secreted and could be immunoprecipitated with the anti-FLAG coupled agarose. In some cases, a doublet is observed for the 30-kDa dimer. We believe that the generally minor upper band represents mature MIC-1 produced as a result of cleavage at an alternative furin-like recognition site located several amino acids upstream of the major cleavage site (*32*). No proteins were recognized from

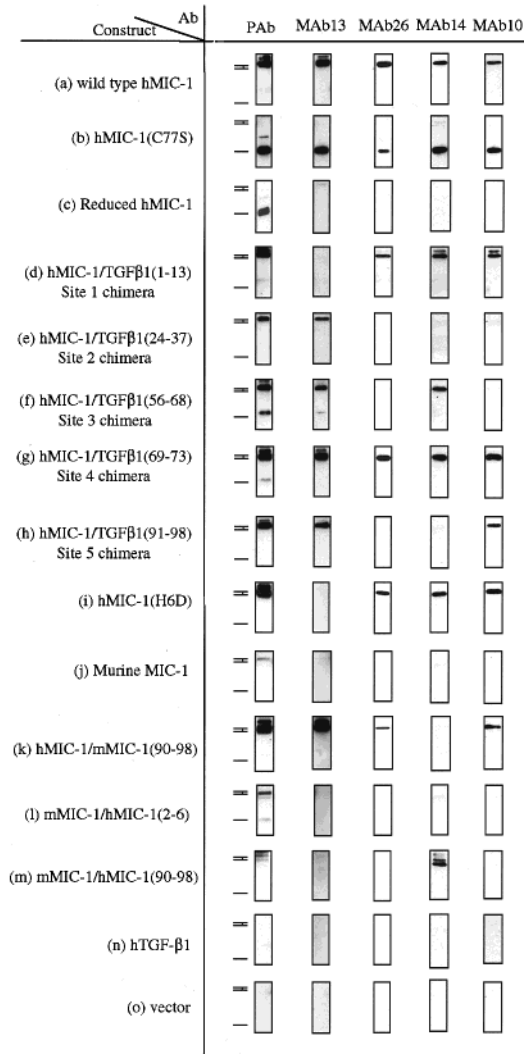

FIGURE 4: Analysis of MAb specificities. Immunoprecipitated wild-type or mutant MIC-1 and TGFβ proteins were electrophoresed under reducing or nonreducing conditions and then blotted onto nitrocellulose. Blots were probed with either polyclonal antiserum (diluted 1:7000) or MAbs (diluted 1:1) as indicated. Protein loads were identical for PAb 233, MAb 13, and MAb 26. Twice as much protein was loaded for MAb 14 and MAb 10. The markers indicate the migration position for the MIC-1 dimer and monomer.

the supernatant of cells transfected with the vector only (Figure 4, row o). The only protein not recognized by any antibody was TGF-β1 (Figure 4, row n), although subsequent probing of the blots with anti-FLAG antibody demonstrated that the protein was secreted (data not shown). Therefore, none of the epitopes for the five antibodies are conserved between hTGF-β1 and hMIC-1, which is not surprising considering the relatively low sequence homology (19% across the seven-cysteine "cystine-knot" domain). Somewhat more surprising however was the fact that none of the monoclonal antibodies recognized the murine MIC-1 protein, and the polyclonal antisera did so only relatively poorly (Figure 4, row j). Human and murine MIC-1 mature regions are 67% identical; therefore, many of the evolutionary amino acid changes have probably occurred in the surface-exposed regions that form the epitopes for the antibodies tested. As antibody epitopes frequently correspond to, or overlap with, receptor binding regions, it will be of interest to examine the receptor specificities and affinities of the murine and human MIC-1 molecules once a suitable assay is available.

Only the polyclonal antibody recognized the reduced protein (Figure 4, row c). This indicates that the epitopes recognized by the monoclonal antibodies are all conformation-dependent, while the polyclonal sera contains antibodies that can also recognize linear epitopes. This is discussed further below. The fact that the construct in which Cys 77 was mutated to a Ser residue was secreted as a 15-kDa protein and which was recognized by all antibodies (Figure 4, row b) strongly supports the prediction that this cysteine residue in MIC-1 forms an interchain disulfide bridge, as does the corresponding cysteine residue in TGF-β1,2,3, activin, and BMP2 and 7.

MAb 13. Monoclonal antibody 13 (in conjunction with PAb 233) is currently being used successfully by us in a sandwich ELISA for the detection of MIC-1 in human serum, conditioned medium, and amniotic fluid (unpublished results). In this assay, MAb 13 is used as the capture antibody and PAb 233 is the detection antibody. The results of the present study have enabled us to localize the epitope and to define at least one key amino acid. All MIC-1/TGF-β1 chimeras were recognized by MAb 13 with the exception of the MIC-1/TGF-β1 site 1 chimera (Figure 4, rows d−h). From this result, we can conclude that the MAb 13 epitope does not involve amino acids from sites 2−5 (i.e., residues 24−37, 56−68, 69−73, 91−98); however, it does involve amino acids at the amino terminus (residues 1−13) of the mature protein that were replaced in the site 1 chimera. Consistent with this result is the observation that the antibody does not recognize the construct in which histidine 6 was changed to an aspartic acid (Figure 4, row i). This demonstrates that MAb 13 can differentiate between the two allelic forms of MIC-1 described above and therefore will be a useful reagent for the analysis of these forms of MIC-1.

Human and murine MIC-1 vary in the amino terminal 13 residues only at positions 2, 3, 4, and 6. As MAb 13 was unable to recognize the murine MIC-1 construct in which residues 2−6 were replaced with the corresponding human sequence (Figure 4, row l), we can conclude that additional residues outside of the amino terminus which differ between the human and mouse proteins are possibly also involved. Furthermore, this epitope (which is conformation-dependent) is probably stabilized by the (noncystine-knot) disulfide bond between residues Cys7−Cys16. In TGF-β, this disulfide bond anchors the amino terminus to the protein core. The very strong recognition of the Cys 77 to Ser "monomer" mutant indicates that the conformation of this region is unchanged by the association of the subunits.

The above results are consistent with the relative spatial arrangement of the regions examined if it is assumed that MIC-1 will adopt a three-dimensional structure similar to that of the other superfamily members for which the structures have been solved. This is illustrated in Figure 5 where it can be seen that the location of the amino terminus and hence the MAb 13 epitope is remote or distinct from the other sites which, when altered, had no effect of antibody binding.

Previous studies have shown that antibodies raised against synthetic peptides corresponding to the amino terminus of TGF-β2 (*22*) and the inhibin α (*23*, *33*) were able neutralize the biological activity of these proteins in various in vitro and in vivo assays. It will therefore be of interest to determine

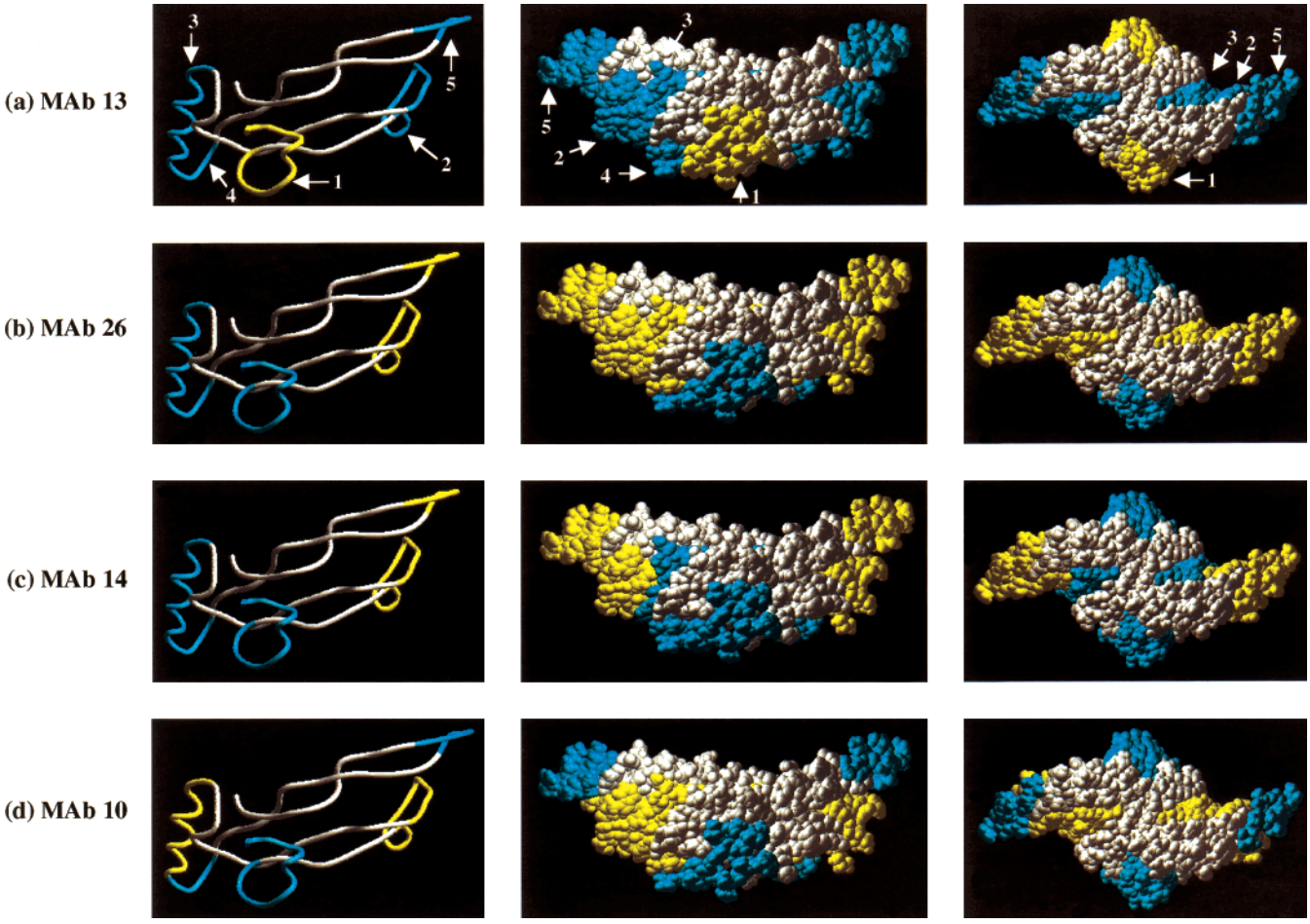

FIGURE 5: MAb specificities in relation to the TGF-β1 three-dimensional structure. The epitopes for the MAbs were mapped onto the three-dimensional structure of TGF-β1 as determined by nuclear magnetic resonance spectroscopy (coordinates derived from the PDB file: 1KLA). Residues in yellow indicate those in MIC-1 which when replaced with the corresponding residues in TGF-β1 abolished binding of the indicated MAb. The residues in blue indicate regions in which MAb binding was unaffected by replacement with the corresponding TGF-β1 residues. The first panel for each antibody represents the carbon backbone for the TGF-β1 monomer; the second panel is a "front-on" view spacefill model of the TGFβ1 dimer, and the third panel is the "top-down" view. Models were generated using the Swiss PDB viewer program. Note that for MAb 26, site 3 is indicated in blue in the monomer and yellow in the dimer reflecting the different behavior of the monomeric and dimeric site 3 chimeras with this antibody.

whether MAb 13 is similarly immunoneutralizing when a suitable assay for MIC-1 is established.

MAb 26. The specificity of MAb 26 appears to differ significantly from that of MAb 13 based upon its cross-reactivity with the various MIC-1/TGF-β chimeras. This antibody was able to bind to the site 1 and site 4 chimeras (Figure 4, rows d and g) but not to the site 2, 3, or 5 chimeras (Figure 4, rows e, f, and h). Furthermore, only relatively weak recognition was observed when site 5 of hMIC-1 was replaced with the corresponding murine sequence (Figure 4, row k), but no binding was observed for the mMIC-1/hMIC-1 site 5 chimera (Figure 4, row m). From these combined results, we can conclude that the epitope does not involve residues 1−13 or 69−73 but does involve residues within the regions 24−37, 56−68, and 91−98.

Because of the disparate location of these three regions within the MIC-1 primary sequence, the conformational dependence of this epitope becomes obvious. Examination of the TGF-β1 three-dimensional structure demonstrates the relative proximity of residues 24−37 (site 2) and 91−98 (site 5) (Figure 5, panel b). These regions, which are located on the tips of the two so-called "fingers", are directly adjacent, and therefore it is not surprising that amino acids from both sites could contribute to the epitope. The lack of involvement of residues 1−13 and 69−73 is also consistent with their location remote from fingertips (Figure 5, panel b). However, residues 56−68, which form the major α-helix within the protein and also appear to be involved in the epitope, are located at the opposite "end" of the monomer to the fingertips. Therefore, it is unlikely that the MAb would cross-react to any degree with the monomer, as it does, if these residues directly contributed to the epitope. It is only in the dimer that the α-helix from one subunit becomes positioned directly adjacent to the "fingertips" on other subunit, and the dimer interface is made up predominantly of hydrophobic residues from the α-helix of one subunit and the fingers of the other subunit (*8*). We therefore propose two hypotheses: either that in the site 3 chimera dimer, residues replaced in the helix from one subunit interfere, perhaps sterically or electrostatically, with the antigen−antibody interaction involving the nearby "fingertip" region on the opposite subunit. Alternatively, the replacement of the MIC-1 α-helix with the corresponding TGF-β1 α-helix disrupts the epitope by altering the arrangement of the β-sheets which form the "fingers", hence altering the relative positions of the "fingertips".

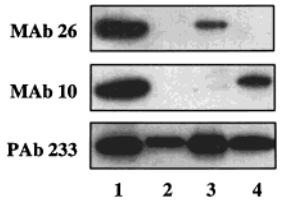

FIGURE 6: Cross-reactivity of MAb 26, MAb 10, and PAb 233 with monomeric chimeras. The wildtype MIC-1 (lane 1) and site 2 (lane 2), site 3 (lane 3), and site 5 (lane 4) chimeras were constructed with a mutation of Cys 77 to Ser resulting in the expression of the monomeric form of the molecules. Immunoprecipitated proteins were electrophoresed under nonreducing conditions and then probed with either MAb 26, Mab 10, or PAb 233. Antibody dilutions and protein loads are exactly as described in the legend for Figure 4. The bands shown migrated with an apparent molecular mass consistent with that of monomeric FLAG-tagged MIC-1 (15 kDa).

Of these two possibilities for the result involving the MIC-1/TGF-β1 site 3 chimera, the first option was most readily investigated. To achieve this, we reconstructed the site 3 chimera with a mutation of Cys 77 to Ser, which resulted in the expression of the monomeric chimera. This site 3 chimera was now recognized by MAb 26 (Figure 6) suggesting that in the dimer, the replacement of the α-helix results in an indirect effect on the epitope located nearby at the fingertips, as suggested in the first hypothesis above. The recognition, however, was also relatively weaker than for the PAb with the same construct indicating that other factors, such as those described in the second hypothesis, may also apply but to a lesser extent. Two other monomeric chimeras (MIC-1/TGFβ1 site 2 and site 5), behaved the same in the monomer as in the dimer, i.e., they did not cross-react (Figure 6).

Amino acid residues from the regions corresponding to both site 2 and site 5 have been shown using site-directed mutagenesis strategies to be important in receptor binding of TGF-β (*12*) and activin A (*14*) as well as GDNF (*15*). In addition, antibodies raised against synthetic peptides that encompass the region corresponding to site 5 in TGF-β1 have been found to be immunoneutralizing both in vitro and in vivo (*18*, *24*). MAb 26 therefore also has the potential to be useful for the modulation of the activity of MIC-1.

MAb 14. The cross-reactivity pattern of MAb 14 was similar to that of MAb 26 in that it was able to recognize the MIC-1/TGF-β site 1 and site 4 chimeras (Figure 4, rows d and g) and failed to recognize both the site 2 and site 5 chimeras (Figure 4e, h), suggesting an involvement of residues in the regions 24−37 and 91−98 on the "fingertips" of the molecule. However, the MAb 14 cross-reactivity pattern was quite different to that of MAb 26 in that it was also able to recognize the MIC-1/TGF-β site 3 chimera (Figure 4, row f) in the dimeric molecule (MAb 26 only recognized the monomeric MIC-1/TGF-β1 site 3 chimera). This result therefore indicates a subtly distinct epitope specificity.

Strong evidence for the location of the MAb 14 epitope is provided by the hMIC-1/mMIC-1 (*90*−*98*) chimera that was not recognized by this antibody (unlike MAb 26) (Figure 4, row k). The murine and human proteins differ only by three residues in this region (hQ90mH, hK91mR, hT94mS) (Figure 2); therefore, at least one of these residues appears to be critical. More compelling, however, is the fact that it was possible to engineer mMIC-1 so that it could be recognized by MAb 14 by replacement of the same three amino acids with the corresponding human residues (Figure 4, row m). In this context, it should be noted that site 2 differs by only one amino acid (hA30mS) between human and murine MIC-1. Together these results indicate that the MAb 14 epitope is most probably dominantly centered on the region corresponding to site 5 (fingertip 2) (Figure 5, panel d). A recent study using an anti-peptide antibody raised to a synthetic peptide that encompasses this fingertip region of MIC-1 has been shown to block the ability of MIC-1 to inhibit MvILu mink lung cell growth (*5*). However, the concentration of MIC-1 (0.8 μg/mL) required was so high as compared to the concentration of TGF-β (20−50 pg/mL) typically used to induce the same effect that the biological relevance of this result is questionable.

MAb 10. As with MAb 26 and MAb 14, MAb 10 also recognized the MIC-1/TGF-β site 1 and 4 chimeras (Figure 4, rows d and g) and failed to bind the site 2 chimera (Figure 4, row e). MAb 10, however, was unlike those other antibodies in that it also recognized the site 5 chimera (Figure 4, row h) but failed to bind the site 3 chimera (Figure 4, row f). It therefore appears that this MAb has a distinct epitope specificity to the previous MAbs described. The cross-reactivity pattern observed with these chimeras suggests that the epitope involves amino acids in the regions 24−37 and 56−68. As discussed above for MAb 26, these regions are located quite distant to one another in the monomer (Figure 5, panel c); therefore, it is unlikely that the MAb would bind to the hMIC-1(C77S) monomer mutant to the extent that it does if there was a direct contribution of amino acids from both sites. The reasons for the lack of binding observed for MAb 26 to the same chimeras therefore possibly also apply for MAb 10, and therefore the cross-reactivity of MAb 10 with the MIC-1/TGF-β1 site 3 monomeric (C77S) chimera was also examined. The results demonstrate that, unlike MAb 26, MAb 10 was still unable to recognize the site 3 chimera in the monomeric form (Figure 6). Its recognition pattern for the site 2 and site 5 monomeric chimeras, however, was the same as in the dimeric form of these proteins (Figure 6). Therefore, we hypothesise that replacement of the α-helix disrupts the MAb 10 epitope in the distant "fingertip" (residues 24−37) by altering the arrangement of the β-sheets that emerge from either end of the helix and which form the "fingers". While this hypothesis is difficult to test, it may be relevant that it has been previously noted that the angle between the α-helix axes in the dimer, as defined by Griffith et al. (*7*), is specific for different subgroups within the superfamily. For example, the BMPs have an interhelical angle of about 48° while in the TGF-β's, it is 37° (*11*). While the significance of this difference is still unknown, our results demonstrate that the introduction of a "foreign" α-helix (i.e., a helix from a different superfamily subgroup) can have a wide ranging effect across the molecule. Furthermore, this effect appears to be more significant in relation to the MAb 10 epitope which involves only the fingertip corresponding to site 2 as compared to the MAb 26 epitope that involves both the site 2 and site 5 fingertips.

Polyclonal Antisera. The polyclonal antiserum was capable of recognizing all of the human MIC-1 mutant constructs (Figure 4, rows d−h and k−m) as well as the reduced protein (Figure 4, row c). This demonstrates that more epitopes exist on MIC-1 than those recognized by the four monoclonal

antibodies that we have generated and characterized above. At least one of these additional epitopes is probably a linear epitope on the basis of the strong cross-reactivity observed with the reduced protein. The relatively strong recognition of all of the mutant constructs by the polyclonal antiserum suggests that there was probably not one epitope that was dominant in generating this particular immune response.

Conclusions. The combined results of this study represent the most thorough epitope mapping study performed on any TGF-β superfamily member to date. There is evidence for the presence of at least five distinct epitope specificities on the surface of MIC-1. At least three of these appear to be partially overlapping because replacement of residues 24−37 affected the binding of all of the MAbs except MAb 13, suggesting that this may be an immunodominant region on MIC-1. It is noteworthy that a previous comprehensive epitope mapping study of the human chorionic gonadotrophin (hCG) α- and β-subunits, which both have cystine knot structures and are approximately the same size as the MIC-1, revealed a similar number of epitopes per subunit (*34*). Significantly, the major immunogenic regions of hCG were located at the tips of the loops of the subunits that are analogous to the "fingers" of MIC-1 on which the majority of the epitopes studied are located. As data from a number of studies has demonstrated that many of the critical residues for receptor binding of TGF-β superfamily proteins are also located on the fingers regions of the protein (*12*, *14*−*16*), it appears that these regions are the major site of molecular recognition/interaction. In this context, the results involving the effect of replacement of the major α-helix in MIC-1 on the epitopes for MAb 26 and MAb 10 were particularly interesting, as they suggest that the orientation or arrangement of the fingertip regions is influenced by the nature of the helix itself. The differences previously observed in interhelical angles for the various superfamily subgroups (see above), therefore, may be an important indirect factor for determining cytokine specificity.

This laboratory is currently investigating the clinical relevance of MIC-1 which requires the use of sensitive and specific immunoassays. The results of the present study, however, have highlighted at least one important factor that must be considered in the development of further assays, namely, that some MAbs may be allele-specific, as MAb 13 was shown to be. This has obvious consequences when, for example, the concentration of MIC-1 in various samples is estimated. Finally, one of the important clinical applications of immunochemical mapping is that it provides a basis for comparison and standardization of results derived from immunoassays between laboratories. As the panel of antigens used in this study readily enabled us to discern each of our four MAb specificities, it should also prove to be useful for the comparison of MIC-1 MAb specificities used in other laboratories, as well as to potentially identify new specificities if and when other MAbs are produced.

REFERENCES

1. Bootcov, M. R., Bauskin, A. R., Valenzuela, S. M., Moore, A. G., Bansal, M., He, X. Y., Zhang, H. P., Donnellan, M., Mahler, S., Pryor, K., Walsh, B. J., Nicholson, R. C., Fairlie, W. D., Por, S. B., Robbins, J. M., and Breit, S. N. (1997) *Proc. Natl. Acad. Sci. U.S.A. 94*, 11514−9.
2. Fairlie, W. D., Moore, A. G., Bauskin, A. R., Russell, P. K., Zhang, H. P., and Breit, S. N. (1999) *J. Leukocyte Biol. 65*, 2−5.
3. Paralkar, V. M., Vail, A. L., Grasser, W. A., Brown, T. A., Xu, H., Vukicevic, S., Ke, H. Z., Qi, H., Owen, T. A., and Thompson, D. D. (1998) *J. Biol. Chem. 273*, 13760−7.
4. Hromas, R., Hufford, M., Sutton, J., Xu, D., Li, Y., and Lu, L. (1997) *Biochim. Biophys. Acta 1354*, 40−4.
5. Tan, M., Wang, Y., Guan, K., and Sun, Y. (2000) *Proc. Natl. Acad. Sci. U.S.A. 97*, 109−114.
6. Daopin, S., Piez, K. A., Ogawa, Y., and Davies, D. R. (1992) *Science 257*, 369−73.
7. Griffith, D. L., Keck, P. C., Sampath, T. K., Rueger, D. C., and Carlson, W. D. (1996) *Proc. Natl. Acad. Sci. U.S.A. 93*, 878−83.
8. Hinck, A. P., Archer, S. J., Qian, S. W., Roberts, A. B., Sporn, M. B., Weatherbee, J. A., Tsang, M. L., Lucas, R., Zhang, B. L., Wenker, J., and Torchia, D. A. (1996) *Biochemistry 35*, 8517−34.
9. Mittl, P. R., Priestle, J. P., Cox, D. A., McMaster, G., Cerletti, N., and Grutter, M. G. (1996) *Protein Sci. 5*, 1261−71.
10. Eigenbrot, C., and Gerber, N. (1997) *Nat. Struct. Biol. 4*, 435−8.
11. Scheufler, C., Sebald, W., and Hulsmeyer, M. (1999) *J. Mol. Biol. 287*, 103−15.
12. Burmester, J. K., Qian, S. W., Ohlsen, D., Phan, S., Sporn, M. B., and Roberts, A. B. (1998) *Growth Factors 15*, 231−42.
13. Huang, S. S., Zhou, M., Johnson, F. E., Shieh, H. S., and Huang, J. S. (1999) *J. Biol. Chem. 274*, 27754−8.
14. Wuytens, G., Verschueren, K., de Winter, J. P., Gajendran, N., Beek, L., Devos, K., Bosman, F., de Waele, P., Andries, M., van den Eijnden-van Raaij, A. J., Smith, J. C., and Huylebroeck, D. (1999) *J. Biol. Chem. 274*, 9821−7.
15. Eketjall, S., Fainzilber, M., Murray-Rust, J., and Ibanez, C. F. (1999) *EMBO J. 18*, 5901−10.
16. Bahloh, R. H., Tansey, M. G., Johnson, E. M., and Milbrandt, J. (2000) *J. Biol. Chem. 275*, 3412−3420.
17. Lucas, C., Fendly, B. M., Mukku, V. R., Wong, W. L., and Palladino, M. A. (1991) *Methods Enzymol. 198*, 303−16.
18. Flanders, K. C., Roberts, A. B., Ling, N., Fleurdelys, B. E., and Sporn, M. B. (1988) *Biochemistry 27*, 739−46.
19. Flanders, K. C., Cissel, D. S., Mullen, L. T., Danielpour, D., Sporn, M. B., and Roberts, A. B. (1990) *Growth Factors 3*, 45−52.
20. Saito, S., Roche, P. C., McCormick, D. J., and Ryan, R. J. (1989) *Endocrinology 125*, 898−905.
21. Tahara, N., Yasumitsu, H., and Umeda, M. (1993) *Hybridoma 12*, 441−53.
22. Van den Eijnden-Van Raaij, A. J., Koornneef, I., Slager, H. G., Mummery, C. L., and Van Zoelen, E. J. (1990) *J. Immunol. Methods 133*, 107−18.
23. Wrathall, J. H., McLeod, B. J., Glencross, R. G., Beard, A. J., and Knight, P. G. (1990) *J. Endocrinol. 124*, 167−76.
24. Hoefer, M., and Anderer, F. A. (1995) *Cancer Immunol. Immunother. 41*, 302−8.
25. Dasch, J. R., Pace, D. R., Waegell, W., Inenaga, D., and Ellingsworth, L. (1989) *J. Immunol. 142*, 1536−41.
26. Danielpour, D., and Roberts, A. B. (1995) *J. Immunol. Methods 180*, 265−72.
27. Lucas, C., Bald, L. N., Fendly, B. M., Mora-Worms, M., Figari, I. S., Patzer, E. J., and Palladino, M. A. (1990) *J. Immunol. 145*, 1415−22.
28. Lambert-Messerlian, G. M., Isaacson, K., Crowley, W. F. Jr., Sluss, P., and Schneyer, A. L. (1994) *J. Clin. Endocrinol. Metab. 78*, 433−9.
29. Fairlie, W. D., Zhang, H.-P., Brown, P. K., Russell, P. K., Bauskin, A. R., and Breit, S. N. (2000) *Gene 254*, 67−76.
30. Fisher, C. L., and Pei, G. K. (1997) *Biotechniques 23*, *570*−*1*, 574.
31. Breit, S. N., and Bootcov, M. R. (1997) Patent PCT/AU96/00386.

32. Bauskin, A. R., Zhang, H.-P., Fairlie, W. D., He, X. Y., Russell, P. K., Moore, A. G., Brown, D. A., Stanley, K. K., and Breit, S. N. (2000) *EMBO J. 19*, 2212−2220.
33. Scanlon, A. R., Sunderland, S. J., Martin, T. L., Goulding, D., O'Callaghan, D., Williams, D. H., Headon, D. R., Boland, M. P., Ireland, J. J., and Roche, J. F. (1993) *J. Reprod. Fertil. 97*, 213−22.
34. Berger, P., Bidart, J. M., Delves, P. S., Dirnhofer, S., Hoermann, R., Isaacs, N., Jackson, A., Klonisch, T., Lapthorn, A., Lund, T., Mann, K., Roitt, I., Schwarz, S., and Wick, G. (1996) *Mol. Cell. Endocrinol. 125*, 33−43.

BI001064P